Impact of the Oxidized Guanine Lesion Spiroiminodihydantoin on the Conformation and Thermodynamic Stability of a 15-mer DNA Duplex[†]

Fadzai Chinyengetere and Elizabeth R. Jamieson*

Department of Chemistry, Smith College, Northampton, Massachusetts 01063

Received July 27, 2007; Revised Manuscript Received November 2, 2007

ABSTRACT: Spiroiminodihydantoin (Sp) is a hyperoxidized guanine base produced from oxidation of the mutagenic DNA lesion 7,8-dihydro-8-oxo-2′-deoxguanosine (8-oxoG) by a variety of species including peroxynitrite, singlet oxygen, and the high-valent metals Ir(IV) and Cr(V). In this study, the conformation and thermodynamic stability of a 15-mer DNA duplex containing an Sp lesion are examined using spectroscopic techniques and differential scanning calorimetry (DSC). The Sp lesion does not alter the global B-form conformation of the DNA duplex as determined by circular dichroism spectroscopy. Thermal denaturation experiments find that Sp significantly lowers the thermal stability of the duplex by ∼20 °C. The enthalpies, entropies, and free energies of duplex formation for 15-mers containing guanine, 8-oxoG, and Sp were determined by performing DSC experiments as well as van't Hoff analysis of UV melting spectroscopic data. The thermodynamic stability of the Sp duplex is significantly reduced compared to that of both the 8-oxoG and parent G duplexes, with the thermodynamic destabilization being enthalpic in origin. The thermodynamic impact of the Sp lesion is compared to what is found for other types of DNA base damage and discussed in relation to how the presence of this lesion could affect cellular processes, in particular the recognition and repair of these adducts by the base excision repair enzymes.

A common factor implicated in aging, neurological disorders, mutagenesis, and carcinogenesis is the oxidation of DNA bases (*1*−*5*). Guanine, the DNA base with the lowest reduction potential (*6*), is easily oxidized to 7,8-dihydro-8-oxo-2′-deoxguanosine (8-oxoG;[1] Figure 1) by numerous DNA-damaging agents. Formation of 8-oxoG, often used as a biomarker for oxidative DNA damage in cells (*7*), causes G·C → T·A transversions (*8*−*10*). Recent experimental evidence suggests that 8-oxoG may not be the final oxidation product of guanine. Rather, 8-oxoG, which has a reduction potential lower than that of guanine, is prone to undergo further oxidation upon exposure to various oxidants including peroxynitrite (*11*−*14*), singlet oxygen (*15*), and the high-valent metals Ir(IV) (*16*) and Cr(V) (*17*), producing lesions such as oxaluric acid, guanidinohydantoin, and spiroiminodihydantoin.

One lesion of particular interest in this group of hyperoxidized guanine lesions is spiroiminodihydantoin (Sp; Figure 1). This lesion is highly mutagenic, producing greater levels of G·C → T·A transversions than 8-oxoG in addition to causing G·C → C·G transversions (*18*−*21*). It also arrests DNA polymerase activity. In terms of biological relevance, researchers exploring the cancer-causing mechanism of Cr(VI) have found the Sp lesion to be of particular interest. Human exposure to hexavalent Cr, usually in the form of chromate, occurs mainly through industrial sources and environmental contamination (*22*−*25*). Facile cellular uptake of chromate by anion transport systems is an important factor in its toxicity. Once inside the cell, Cr(VI) is reduced to Cr(III) by species such as glutathione, cysteine, and ascorbate. During this intracellular reduction, high-valent Cr(V) and Cr(IV) compounds as well as carbon- and oxygen-based radical species are generated, all of which can oxidatively damage DNA. Recently, the Sp lesion has been shown to accumulate in base excision repair deficient *Escherichia coli* cells treated with Cr(VI) (*26*), and when double-stranded DNA was treated with Cr(VI) and ascorbate in vitro, the concentration of Sp lesions found on the DNA was ∼20 times greater than that of 8-oxoG (*27*). Most interestingly, the G·C → T·A and G·C → C·G transversions observed with this lesion correspond to the mutations typically found in human lung tumors from chromate-exposed workers (*28*, *29*), suggesting a connection between Sp lesions and Cr(VI) carcinogenesis.

To date, relatively little is known about the impact of the Sp lesion on the structure and stability of duplex DNA. The Sp base contains a tetrahedral carbon atom whose *R* and *S* stereoisomers form diasteriomers when bonded to the furanose moiety of DNA. Computational studies have revealed that the two rings of the Sp base are nearly orthogonal to each other and that the Sp stereoisomers favor positioning in the major groove of B-form DNA (*30*, *31*). In addition, formation of Sp is predicted to disrupt Watson−Crick hydrogen bonding and base stacking around the lesion and causes groove widening, resulting in a destabilized helix

[†] Funding for this work was provided by Smith College (Tomlinson Fund and Howard Hughes Medical Institute Awards to F.C., Start-up Funds and CFCD Awards to E.R.J.). Mass spectral data were obtained at the University of Massachusetts Mass Spectrometry Facility, which is supported, in part, by the National Science Foundation.

* To whom correspondence should be addressed. Phone: (413) 585-7588. Fax: (413) 585-3786. E-mail: ejamieso@email.smith.edu.

[1] Abbreviations: Sp, spiroiminodihydantoin; 8-oxoG, 7,8-dihydro-8-oxo-2′-deoxyguanosine; DSC, differential scanning calorimetry; CD, circular dichroism; BER, base excision repair.

10.1021/bi701502t CCC: $40.75
Published on Web 02/19/2008

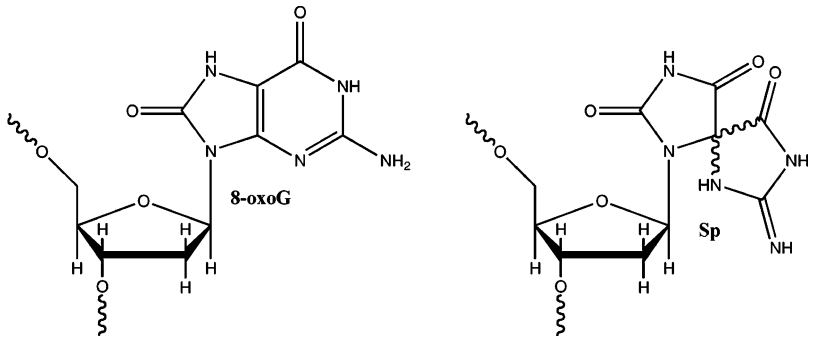

FIGURE 1: Structures of the oxidized guanine lesions 7,8-dihydro-8-oxo-2′-deoxguanosine (8-oxoG) and spiroiminodihydantoin (Sp).

structure. UV melting studies analyzing equilibrium melting curves demonstrated a significant destabilization of the DNA helix (3.6−6.7 kcal/mol) in the presence of the Sp lesion (*18*, *32*). The degree of helix destabilization was dependent on the DNA sequence context of the Sp lesion as well as its base pairing partner in the complementary strand.

The current study provides detailed thermodynamic data to more fully characterize the energetic impact of oxidizing a guanine base to Sp on a DNA duplex. Circular dichroism (CD), differential scanning calorimetry (DSC), and concentration-dependent UV thermal denaturation studies were carried out to examine the conformation, thermal stability, and energetics of 15-mer DNA duplexes containing unmodified guanine, 8-oxoG, or Sp. These investigations reveal a hierarchy in the thermal and thermodynamic stabilities of the three sequences of G·C > 8-oxoG·C ≫ Sp·C, with the Sp lesion being significantly more destabilizing to the duplex than 8-oxoG. This study presents a model-independent thermodynamic characterization of the Sp lesion, providing a better understanding of the energetic consequences of forming this lesion and insight into how this might affect biological processes such as DNA damage recognition and repair.

EXPERIMENTAL PROCEDURES

Reagents. HPLC-purified 15-mer oligonucleotides containing standard DNA bases were purchased from Integrated DNA Technologies (IDT), and HPLC-pure 8-oxoG-containing oligonucleotides were obtained from Trilink Biotechnologies. Sodium hexachloroiridate(IV) hexahydrate ($Na_2IrCl_6 \cdot 6H_2O$) was purchased from Acros Organics. Acetonitrile (HPLC grade) and sodium chloride were obtained from Fisher. Ammonium acetate and EDTA were purchased from USB, while sodium phosphate dibasic (Na_2HPO_4; ACS reagent) and sodium phosphate monobasic monohydrate ($NaH_2PO_4 \cdot H_2O$; ACS reagent) were obtained from Sigma-Aldrich.

Synthesis of the Sp Lesion. The Sp lesion was synthesized by oxidizing an 8-oxoG-containing oligonucleotide with sodium hexachloroiridate(IV) hexahydrate ($Na_2IrCl_6 \cdot 6H_2O$) (*18*). The 8-oxoG-containing oligonucleotide (12 μM) was reacted with 100 μM $Na_2IrCl_6 \cdot 6H_2O$ in 10 mM sodium phosphate buffer (pH 6.98) and 100 mM sodium chloride. The reaction mixture was heated at 65 °C for 30 min and quenched with 20 mM EDTA (pH 8.0). After quenching, the reaction solution was dialyzed (3500 MWCO) against ddH_2O and lyophilized to dryness.

The Sp lesion was purified on an HP series 1100 HPLC instrument by using a Dionex DNAPac PA-100 9 × 250 mm anion exchange column with a linear gradient from 70% mobile phase A (10% aqueous acetonitrile)/30% mobile phase B (90% 1.5 M ammonium acetate, pH 6, 10% acetonitrile) to 100% mobile phase B over the course of 50 min with a flow rate of 2.5 mL/min (*27*). The two diastereoisomers of the Sp lesion eluted at approximately 30 min (peak 1) and 31 min (peak 2), respectively. The two peaks were collected separately, dialyzed (3500 MWCO) against ddH_2O, and lyophilized. The samples were then characterized by using MALDI-TOF mass spectrometry. The mass spectrum for both peaks 1 and 2 showed the characteristic (M + 16) peak observed for Sp lesions (*16*). The mass spectrum of peak 1 also contained a significant amount of an impurity (M − 51 mass) which has yet to be identified. Consequently, only the pure disasteriomer collected from peak 2 was used to conduct thermodynamic studies.

Annealing of the Oligonucleotide Strands. Each of the oligonucleotides was annealed to the complementary strand before CD, UV melting, or DSC experiments were performed. The concentrations of single-stranded oligonucleotides were determined spectrophotometrically using molar extinction coefficients calculated with nearest neighbor parameters (*33*−*36*). Strands were mixed in a 1:1 ratio in sodium phosphate buffer (10 mM sodium phosphate, pH 6.98, 100 mM NaCl, and 0.1 mM EDTA), heated to 90 °C for ∼3 min, and slowly cooled to room temperature. To confirm that annealing had taken place and that there was no excess single-stranded material, each sample was analyzed by using HPLC with a Dionex DNAPac PA-100 4 × 250 mm column with a linear gradient from 90% mobile phase A (10% aqueous acetonitrile)/10% mobile phase B (90% 1.5 M ammonium acetate, pH 6.0, 10% acetonitrile) to 100% mobile phase B over 26 min at a flow rate of 1 mL/min (*27*).

CD Spectropolarimetry. CD experiments were performed on a Jasco J-715 spectropolarimeter at both 15 and 20 °C using a cell with a 0.1 cm path length. Spectra were recorded from 220 to 320 nm with a 0.2 nm step resolution and a scan rate of 20 nm/min. Oligonucleotide samples were prepared in sodium phosphate buffer (10 mM sodium phosphate, pH 6.98, 100 mM NaCl, and 0.1 mM EDTA) at a duplex concentration of 8 μM.

UV Spectroscopy and Thermal Denaturation Studies. UV spectroscopy was performed on an HP 8452A diode array spectrophotometer using quartz cells with path lengths of 0.1, 0.2, or 1 cm. All samples were prepared in sodium phosphate buffer (10 mM sodium phosphate, pH 6.98, 100 mM NaCl, and 0.1 mM EDTA) with duplex concentrations ranging from 0.5 to 10 μM. Prior to thermal denaturation,

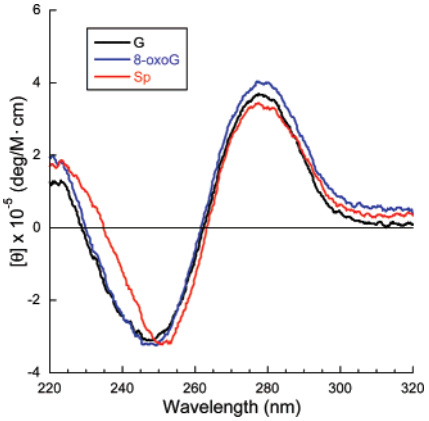

FIGURE 2: Circular dichroism spectra at 20 °C for the G (black), 8-oxoG (blue), and Sp (red) 15-mer DNA duplexes.

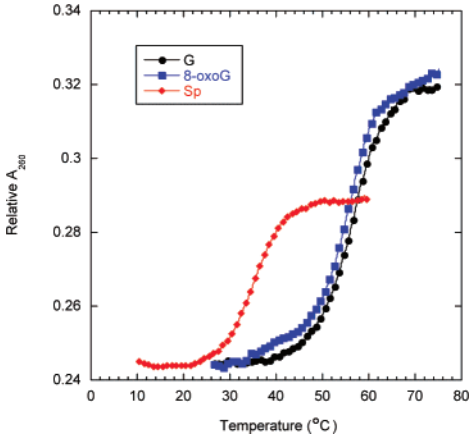

FIGURE 3: UV melting profiles at 260 nm for the G (black), 8-oxoG (blue), and Sp (red) 15-mer duplexes at 1 μM duplex concentration. The melting curves were normalized to produce identical absorbances at initial temperatures for clarity of presentation.

samples were degassed for ~15 min. Thermal denaturation was performed from 25 to 75 °C for the unmodified G and 8-oxoG duplexes; the Sp lesion samples were run from 10 to 65 °C. Absorbance versus temperature profiles were monitored at 260 nm, and the temperature was ramped at a rate of 0.5 °C/min with a hold time of 1 min at each temperature setting. The melting temperature (T_m) for each sample was determined following previously reported procedures (*37*, *38*). A van't Hoff analysis was performed to determine $\Delta H°_{vH}$ and $\Delta S°_{vH}$ from the concentration-dependent UV melting curves (*37*, *38*), and the equation $\Delta G° = \Delta H° - T\Delta S°$ was used to compute the change in the free energy ($\Delta G°_{vH}$).

Differential Scanning Calorimetry. Differential scanning calorimetry experiments were conducted on a model 6300 NanoDSCIII differential scanning calorimeter with a cell volume of 0.334 mL (Calorimetry Sciences Corp.). A sample of each duplex (50 μM) was prepared in sodium phosphate buffer (10 mM sodium phosphate, pH 6.98, 100 mM NaCl, and 0.1 mM EDTA) and dialyzed (mini dialysis kit, Amersham Biosciences, 1000 MWCO) overnight against excess sodium phosphate buffer to equilibrate the buffer and sample solution. Solutions were degassed for ~10 min, and excess heat capacity (C_p^{ex}) versus temperature curves were measured from 10 to 90 °C with a heating/cooling rate of 1 °C/min. The program CpCalc was used to calculate the thermodynamic parameters ΔH_{cal} and ΔS_{cal}. The standard free energy change for binding at 37 °C ($\Delta G^{°37}_{cal}$) was determined as previously described (*39*, *40*).

RESULTS AND DISCUSSION

Examination of the Duplex Conformation Using CD Spectropolarimetry. CD spectropolarimetry was used to investigate the global conformation of the 15-mer duplexes containing G, 8-oxoG, and the Sp lesion (Figure 2). While there are some differences between the samples, overall the spectral shapes for all three duplexes are characteristic of B-form DNA. Previous studies determined that the presence of an 8-oxoG lesion does not alter the global B-form structure of oligonucleotides (*41*). Our results show similar spectra for G and 8-oxoG samples, consistent with the minimal spectral perturbations observed for the G·C and 8-oxoG·C oligonucleotides in those earlier studies. The spectrum for the Sp oligonucleotide, while still indicative of a global B-form DNA conformation, displays a shift to longer wavelengths in the spectral minimum around 250 nm and in the crossover point around 260 nm. Spectral shift toward longer wavelength at this crossover point can be indicative of DNA denaturation (*42*). However, these features are also observed in CD spectra taken at 15 °C, which is well below the melting temperature of the duplex. Thus, while Sp may not alter the global conformation of the duplex, the observed spectral shifts may indicate that there are some differences in DNA structure induced by the Sp lesion.

Effect of the Sp Lesion on the Thermal Stability of the Duplex. Melting curves for the 15-mer duplexes at 1 μM containing G, 8-oxoG, and Sp are presented in Figure 3. These data quite clearly show the significant difference in the melting temperature of the Sp duplex compared to the unmodified guanine and 8-oxoG lesion duplexes. Comparison of the T_m values for the lesions with those of the unmodified guanine at the same concentration provides information about the thermal stability of the duplex. As expected, for all the sequences studied, as the concentration increased, so did the melting temperature. The DNA duplex containing the unmodified guanine was the most thermally stable as it has the highest T_m value at all concentrations examined. The T_m of the 8-oxoG duplex was very similar to that of the control G duplex at all concentrations, consistent with small melting temperature differences observed in earlier studies (*18*, *41*). Consequently, our results demonstrate that duplexes containing 8-oxoG are not significantly more thermally destabilized when compared to the parent G sample. In contrast, our studies definitively show that both the G and 8-oxoG duplexes are significantly more thermally stable than the Sp lesion, which has T_m values ~20 °C lower at all concentrations. In addition, the extent of melting hyperchromism was reduced in the Sp lesion samples, which may indicate perturbations such as unstacking in the initial DNA duplex structure (*43*). Reduction of the DNA melting temperature with Sp lesions has been observed previously for 18-mer template/16-mer primer duplexes (*18*). In those studies, the Sp·C base pair was positioned three bases away from one end of the duplex. The presence of Sp reduced the melting temperature from the parent G·C duplex by 7.6−12.9 °C, depending on the DNA sequence context. Thus, from those results and ours, it is quite clear that the Sp lesion

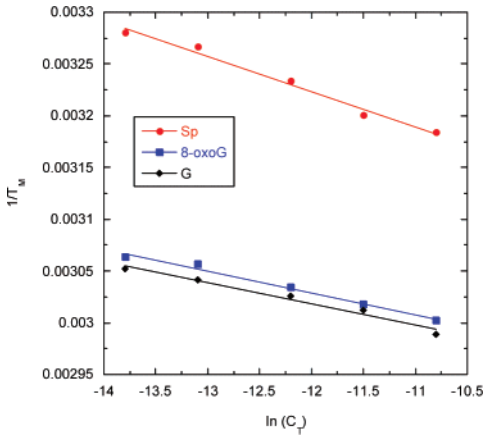

FIGURE 4: van't Hoff plots showing the concentration dependence of the melting temperature for the G (black), 8-oxoG (blue), and Sp (red) 15-mer duplexes.

significantly thermally destabilizes DNA, with differences in the magnitude of this effect being dependent upon the DNA sequence context and the position of the lesion within the strand.

Concentration-Dependent Thermal Denaturation Studies. Differences in the thermal stability of a DNA duplex do not always correlate to changes in its thermodynamic stability (*41*, *44*). Therefore, to investigate the thermodynamic effects of the Sp and 8-oxoG lesions, a series of UV thermal denaturation experiments were performed. Concentration-dependent UV melting curves can be used to establish ΔH°_{vH} and ΔS°_{vH} using van't Hoff analysis that assumes a two-state model (*37*, *38*). By plotting $1/T_m$ against $\ln(C_T)$, the enthalpy and entropy for the bimolecular association of single strands can be calculated according to the equation

$$\frac{1}{T_m} = \frac{R}{\Delta H^\circ_{vH}} \ln(C_T) + \frac{\Delta S^\circ_{vH} - 1.39R}{\Delta H^\circ_{vH}}$$

where C_T is the total strand concentration and R refers to the gas constant. Figure 4 shows the linear plots for the three duplexes. The T_m hierarchy described above holds throughout the concentration range since the lines for the duplexes do not cross (*45*). The more thermally stable sequences are at the bottom of Figure 4, emphasizing the overall thermal stabilities of the duplexes as G > 8-oxoG ≫ Sp.

Table 1 shows the ΔH°_{vH} and ΔS°_{vH} for helix formation obtained for all three duplexes using van't Hoff analysis. It is clear from these data that both the 8-oxoG and Sp lesions enthalpically destabilize the duplex, increasing the duplex transition enthalpy by 3 and 39 kcal/mol, respectively. As with the melting temperatures, the magnitude of the destabilization observed with the Sp lesion is significantly greater than what is seen with 8-oxoG. In contrast, both the 8-oxoG and Sp lesions entropically stabilize the duplex. This phenomenon, often referred to as "enthalpy−entropy compensation", is characteristic of melting transitions of duplex nucleic acids containing lesions and indeed a wide variety of biological systems featuring multiple, weak interactions (*46*−*48*). When this occurs, favorable entropic effects offset some of the free energy penalty for the duplex destabilization (*49*), as depicted in Figure 5. The entropic stabilization observed is consistent with greater disorder for the Sp and 8-oxoG lesions in the duplex state compared to the unmodified guanine sequence.

Values for the change in the free energy (ΔG°_{vH}) at the physiologically relevant temperature 37 °C were calculated using the ΔH°_{vH} and ΔS°_{vH} data (Table 1). Inspection of these data shows that unmodified guanine is the most thermodynamically stable duplex while the helix with the Sp lesion is the least stable, correlating with the hierarchy that was obtained for the thermal stabilities of the respective duplexes. Formation of the 8-oxoG duplex is only slightly less thermodynamically favorable compared to that of the duplex with unmodified guanine. In contrast, the Sp lesion causes significant thermodynamic destabilization ($\Delta\Delta G^\circ_{vH} = 7$ kcal/mol) when compared to the parent G duplex. These results demonstrate that not only is the Sp lesion detrimental to the thermal stability of the duplex, but it also greatly affects the thermodynamic stability of the DNA helix.

Differential Scanning Calorimetry. The van't Hoff analysis described above assumes a two-state model; the two strands are either completely annealed into a duplex or completely denatured into the respective single strands (*37*, *38*). DSC, on the other hand, is a model-independent technique where the excess heat capacity (C_p^{ex}) is plotted against the temperature (T); the area under the curve is ΔH_{cal} (*37*, *38*). The entropy change, ΔS_{cal}, can be obtained from plots of C_p^{ex}/T vs T. Plots of C_p^{ex} versus temperature for the three duplexes studied are given in Figure 6. Consistent with the thermal denaturation experiments, the transition point maximum for the Sp lesion occurs at a position ∼20 °C lower than those for the unmodified G and 8-oxoG duplexes.

The calorimetrically determined ΔH_{cal} and ΔS_{cal} values as well as the ΔG°_{cal} values at 37 °C derived from the DSC experiments are presented in Table 1. As observed with the van't Hoff data, there is an enthalpic destabilization of the helix for 8-oxoG and Sp lesions that is mitigated by an entropic stabilization. Overall, these results yield the same hierarchy in thermodynamic stability observed with van't Hoff analysis. The DSC data find that the unmodified guanine duplex is the most thermodynamically stable with a $\Delta G^{\circ 37}_{cal}$ for formation of the helix of −15.4 kcal/mol, whereas the duplex with the Sp lesion is the least stable, having a significant increase in the free energy of formation of 7.8 kcal/mol.

Model-Independent versus Model-Dependent Data. Comparison of the DSC measurements versus those obtained from van't Hoff analysis allows one to determine how well the three duplexes fit the two-state model. When the helix melting proceeds in a two-state manner, $\Delta H_{vH} \approx \Delta H_{cal}$. Analysis of our data finds that, within the limits of experimental error, $\Delta H_{vH} \approx \Delta H_{cal}$ for both the unmodified guanine and 8-oxoG duplexes, consistent with previous results (*41*, *43*). This is not the case with the Sp lesion, where ΔH_{vH} is at least 12 kcal/mol greater than ΔH_{cal}. Situations where $\Delta H_{vH} > \Delta H_{cal}$ can indicate the presence of multimolecular (aggregation) processes; however, such data for other lesion-containing duplexes have been interpreted as reflecting differences in helix initiation (*49*). The inequality between the van't Hoff and calorimetrically derived enthalpy values in our system may result from the ability of this lesion to act as a barrier to the propagation of interactions necessary for cooperative melting (*43*, *50*).

Table 1: Thermodynamic Parameters for the Formation of the G, 8-oxoG, and Sp 15-mer Duplexes from UV Melting and DSC Experiments

duplex	$\Delta H°_{vH}$ (kcal/mol)	$\Delta S°_{vH}$ [cal/(K·mol)]	$\Delta G°^{37}_{vH}$ (kcal/mol)	ΔH_{cal} (kcal/mol)	ΔS_{cal} [cal/(K·mol)]	$\Delta G°^{37}_{cal}$[a] (kcal/mol)
G	−97 ± 9	−271 ± 25	−13 ± 2	−107 ± 2	−316 ± 5	−15.4 ± 0.3
8-oxoG	−94 ± 7	−265 ± 18	−12 ± 1	−84 ± 2	−250 ± 4	−13.0 ± 0.3
Sp	−58 ± 4	−167 ± 12	−6 ± 1	−41 ± 1	−130 ± 3	−7.6 ± 0.2

[a] $\Delta G°^{37}_{cal}$ values were derived from DSC data following the procedures of Chakrabarti and Schwarz (*40*).

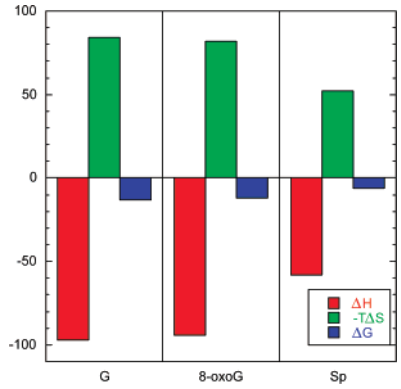

FIGURE 5: Enthalpy−entropy compensation in the 15-mer duplexes. The thermodynamic parameters for the formation of the helices have units of kilocalories per mole. For each sample, $\Delta H°$ values are plotted in red, $-T\Delta S°$ values are in green, and $\Delta G°$ values are in blue.

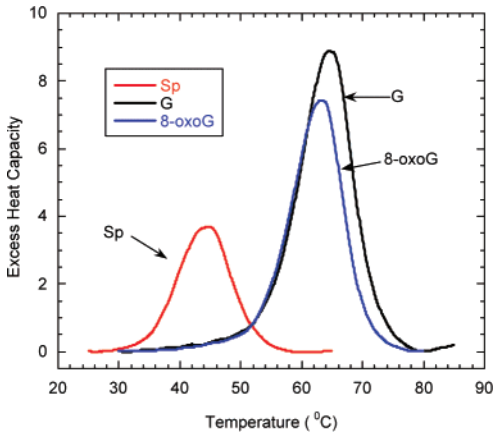

FIGURE 6: DSC thermograms for the G (black), 8-oxoG (blue), and Sp (red) 15-mer duplexes.

Comparison of the Thermodynamic Impact of the Sp Adduct to That of Other DNA Base Lesions. Previous to this study, the only thermodynamic data available for Sp were extracted from UV melting curves of 14- and 16-mer oligonucleotides annealed to 18-mer templates obtained at a single duplex concentration (*18*, *32*). In those studies, ΔG values for formation of the Sp·C duplex at 37 °C for the 16-mer/18-mer samples increased by 3.6−6.7 kcal/mol compared to that of the parent G·C duplex. Both of the duplexes studied showed a significant thermodynamic destabilization, with the extent of the effect being dependent on the DNA sequence context. In our DSC experiments, the $\Delta G°$ of formation for the 15-mer Sp duplex was raised 7.8 kcal/mol above that of the corresponding G·C duplex at 37 °C. Thus, it is clear from both of these studies that the Sp lesion causes a significant thermodynamic destabilization of the DNA helix at physiologically relevant temperatures that may contribute to harmful biological effects.

To provide some perspective on the thermodynamic impact of the Sp lesion in biological systems, the differential free energy values ($\Delta\Delta G$) at 37 °C for a variety of DNA base adducts, compiled from calorimetric and spectroscopic studies, are presented in Table 2. Formation of 8-oxoG, a standard biomarker for oxidative damage in cells (*7*), is by far the least destabilizing of the lesions surveyed, with an average $\Delta\Delta G^{37}$ value of ∼1.5 kcal/mol. This free energy difference corresponds to an equilibrium preference for the G·C duplex over the 8-oxoG·C duplex of about 11:1. Somewhat more destabilizing than 8-oxoG is the exocyclic guanine adduct 1,*N*2-propano-2′-deoxyguanosine, which is produced from α,*β*-unsaturated carbonyl compounds such as acrolein (*51*). In contrast to the relatively small thermodynamic impact of 8-oxoG and 1,N^2-propano-2′-deoxyguanosine, the Sp and the 1,2-intrastrand adducts of the anticancer drug cisplatin display a relatively large average $\Delta\Delta G^{37}$ value of ∼6 kcal/mol. Here, the differential free energy value corresponds to an equilibrium preference for the G·C duplex of ∼17000:1. It is interesting to note that both the Sp and cisplatin lesions show very clear examples of the large effect the DNA sequence context can play on the thermodynamic impact of a lesion, as both have one sequence where the $\Delta\Delta G^{37}$ value is comparable to those found for 8-oxoG and 1,N^2-propano-2′-deoxyguanosine. Studies are currently under way in our laboratory to examine the effect of both DNA sequence context and base pairing partner on the thermodynamic impact of the Sp lesion. The most destabilized lesion in this survey, on the basis of $\Delta\Delta G^{37}$ values, is 3,N^4-deoxyethenocytosine, which can arise from exposure to vinyl chloride, hepatic copper poisoning, or reaction of DNA with products of lipid peroxidation (*49*). This adduct very dramatically reduces the thermodynamic stability of the duplex with a $\Delta\Delta G^{37}$ of 15 kcal/mol, representing a ∼85% loss in the total duplex thermodynamic stability (*49*).

Biological Significance of Thermodynamic Data. To date there are no experimentally obtained structural data for DNA duplexes containing an Sp lesion. Computational studies have been performed to examine the structural impact of the Sp lesion on DNA structure (*31*). These studies find that both Sp stereoisomers prefer the *syn* conformation and have their lowest energy when positioned in the major groove of B-DNA. There are severe distortions in the DNA duplex in the presence of the Sp lesion, resulting from decreased hydrogen-bonding and stacking interactions for Sp and its neighboring bases. This predicted disruption of stacking interactions should be enthalpically unfavorable (*43*), correlating well with the experimental data presented here. The extent of helix distortion is influenced by the base paired with the Sp lesion, with the stability decreasing in the following order: G > A ≈ C > T (*31*). The Sp lesion has a pseudo-thymine hydrogen-bonding conformation; pairing

Table 2: Impact of Various DNA Base Lesions on the Free Energy of Helix Formation at 37 °C[a]

adduct	sequence	$\Delta\Delta G^{37}$ (kcal/mol)	ref
Sp	5′-ACTGATAGACGCACT-3′ 3′-TGACTATCTGCGTGA-5′	7.8	this work
Sp	5′-GACCGGGTCAGTGCTACT-3′ 3′-GGCCCAGTCACGATGA-5′	6.7	*18*
Sp	5′-GATTGAATCAGTGCTACT-3′ 3′-AACTTAGTCACGATGA-5′	3.6	*18*
8-oxoG	5′-ACTGATAGACGCACT-3′ 3′-TGACTATCTGCGTGA-5′	2.4	this work
8-oxoG	5′-GCGTACGCATGCG-3′ 3′-CGCATGCGTACGC-5′	1.8	*41*
8-oxoG	5′-GACCGGGTCAGTGCTACT-3′ 3′-GGCCCAGTCACGATGA-5′	1.0	*18*
8-oxoG	5′-GATTGAATCAGTGCTACT-3′ 3′-AACTTAGTCACGATGA-5′	0.9	*18*
1,N^2-propano-2-deoxyguanosine	5′-CGCATGGGTACGC-3′ 3′-GCGTACCCATGCG-5′	3.5	*51*
cisplatin	5′-CCTCTCTGGTTCTTC-3′ 3′-GGAGAGACCAAGAAG-5′	7.3	*50*
cisplatin	5′-CCTCTCCGGCTCTTC-3′ 3′-GGAGAGGCCGAGAAG-5′	7.5	*50*
cisplatin	5′-CCTCTCAGGATCTTC-3′ 3′-GGAGAGTCCTAGAAG-5′	2.1	*50*
3,N^4-deoxyethenocytosine	5′-CGCATGCGTACGC-3′ 3′-GCGTACGCATGCG-5′	15	*49*

[a] The location of the base lesion is underlined. $\Delta\Delta G$ values are calculated as ΔG^{37}(lesion) − ΔG^{37}(unmodified).

of *syn* Sp with a purine presents less strain than pairing with a pyrimidine, correlating with the prevalence of G·C → T·A and G·C → C·G transversions observed experimentally (*18*−*21*). In sum, the calculational studies predict helices containing an Sp lesion to have a distorted structure with widening of the major groove, diminished quality of the Watson−Crick base pairing, and weakened stacking interactions. These structural factors should decrease the thermal and thermodynamic stability of a DNA duplex, consistent with the results observed in our study.

In cells, Sp lesions are recognized and repaired by enzymes in the base excision repair (BER) pathway such as the bacterial Nei enzyme (*52*) and mammalian NEIL (Nei-like) DNA glycosylases (*53*). Experimental evidence suggests that BER enzymes move processively along the DNA helix, patrolling for DNA damage (*54*−*57*). When a specific base lesion is encountered, it is rotated 180° from the base pair stack into the active site of the enzyme (a process known as "base flipping") where the glycosidic bond is cleaved (*58*−*61*). The abasic site produced in this reaction is subsequently repaired, restoring the integrity of the DNA molecule (*62*).

Several models have been put forward to describe how these enzymes find damaged bases in the DNA duplex. Verdine and colleagues have suggested that DNA glycosylases actively scan the DNA duplex, flipping each base into the enzyme active site while traveling along the helix (*54*). Alternatively, others have proposed that these proteins rely on a passive extrahelical recognition mechanism, trapping damaged bases that are exposed during spontaneous DNA breathing (*63*). In the "pinch−push−pull" mechanism suggested by Tainer *et al.*, the enzymes bend the DNA backbone (*64*). This "pinching" action precedes the "push and pull" motions used to flip the base lesion out of the helix. Finally, the Barton group has proposed a DNA-mediated charge transport (CT) mechanism (*65*). Many BER enzymes, including MutY, which recognizes 8-oxoG·A mismatches, contain $[Fe_4S_4]^{2+}$ clusters (*66*). In this model, the ability of a BER enzyme to bind DNA and repair damage is modulated by the redox state of the $[Fe_4S_4]$ cluster, controlled through DNA CT.

Although structural features are important for the specific recognition of base lesions in the active site (*62*), energetics may also play a key role in identifying DNA damage (*41*, *44*, *67*). Duplexes containing an 8-oxoG·C base pair are structurally very similar to the ones containing the standard G·C base pair (*68*, *69*). Consequently, it is unlikely that repair enzymes recognize 8-oxoG by structural means alone (*41*). The thermodynamic instability caused by a DNA lesion may aid in the recognition of DNA damage by BER enzymes. A common feature among many different DNA base lesions, including the Sp and 8-oxoG examined here, is the enthalpically driven thermodynamic destabilization of the helix (*41*, *43*, *49*, *51*). Reduction of the duplex stability should make it easier for recognition of the damage to occur in all of the models presented above (*70*). For example, less stable DNA should be more flexible and therefore easier to "pinch" or actively scan. It should also have a greater propensity to produce the extrahelical bases required in the passive model. Disruption of stacking interactions, such as the kind that would inhibit DNA CT, is enthalpically unfavorable, consistent with our results. Thus, the thermodynamic study of a base lesion can not only supply information on the energetic consequences of adduct formation, but also provide insight into the process of recognition and repair by BER proteins.

CONCLUSIONS

The impact of the Sp lesion on the conformation, thermal stability, and energetics of the DNA duplex was examined in this study. Results from our circular dichroism experiments find that the Sp lesion does not induce a global conformational change from B-form DNA. Data from both our van't Hoff UV melting spectroscopic and DSC studies reveal that

the Sp lesion significantly lowers both the thermal and thermodynamic stability of the helix, with the thermodynamic destabilization being enthalpic in origin. This lesion displays the enthalpy−entropy compensation that is common among several other DNA base lesions. Most interestingly, the extent of thermal and thermodynamic destabilization observed with the Sp lesion is far greater in magnitude than what is observed with the standard marker for oxidative DNA damage, 8-oxoG, suggesting that the Sp lesion may be even more detrimental to biological systems.

ACKNOWLEDGMENT

Mass spectral data were obtained by Dr. Steve Eyles at the University of Massachusetts Mass Spectrometry Facility. We thank Prof. Stylanios Scordilis (Smith), Dr. Charles Amass (Smith), Prof. Lila Gierasch (UMass), and Dr. Jiang Hong (UMass) for access to and assistance with instrumentation and Prof. Megan Nunez (Mt. Holyoke) for helpful discussions.

REFERENCES

1. Wiseman, H., and Halliwell, B. (1996) Damage to DNA by reactive oxygen and nitrogen species: Role in inflammatory disease and progression to cancer, *Biochem. J. 313*, 17−29.
2. Gotz, M. E., Kunig, G., Riederer, P., and Youdim, M. B. H. (1994) Oxidative stress: free radical production in neural degeneration, *Pharmacol. Ther. 63*, 37−122.
3. Finkel, T., and Holbrook, N. J. (2000) Oxidants, oxidative stress and the biology of ageing, *Nature 408*, 239−247.
4. Feig, D. I., and Loeb, L. A. (1994) Oxygen radical induced mutagenesis is DNA polymerase specific, *J. Mol. Biol. 235*, 33−41.
5. Ames, B. N., Shigenaga, M. K., and Hagen, T. M. (1993) Oxidants, antioxidants and the degenerative disease of aging, *Proc. Natl. Acad. Sci. U.S.A. 90*, 7915−7922.
6. Steenken, S., and Jovanovic, S. V. (1997) How easily oxidizable is DNA? One-electron reduction potentials of adenosine and guanosine radicals in aqueous solutions, *J. Am. Chem. Soc. 119*, 617−618.
7. Shigenaga, M. K., Aboujaoude, E. N., Chen, Q., and Ames, B. N. (1994) Assays of oxidative DNA damage biomarkers 8-oxo-2′-deoxyguanosine and 8-oxoguanine in nuclear DNA and biological fluids by high-performance liquid chromatography with electrochemical detection, *Methods Enzymol. 234*, 16−33.
8. Wood, M. L., Esteve, A., Morningstar, M. L., Kuziemko, G. M., and Essigmann, J. M. (1992) Genetic effects of oxidative DNA damage: comparative mutagenesis of 7,8-dihydro-8-oxoguanine and 7,8-dihydro-8-oxoaadenine in *Escherichia coli*, *Nucleic Acids Res. 20*, 6023−6032.
9. Moriya, M., Ou, C., Bodepudi, V., Johnson, F., Takeshita, M., and Grollman, A. P. (1991) Site-specific mutagenesis using a gapped duplex vector: a study of translesion synthesis past 8-oxodeoxyguanosine in *E. coli*, *Mutat. Res. 254*, 281−288.
10. Grollman, A. P., and Moriya, M. (1993) Mutagenesis by 8-oxoguanine: an enemy within, *Trends Genet. 9*, 246−249.
11. Tretyakova, N. Y., Niles, J. C., Burney, S., Wishnok, J. S., and Tannenbaum, S. R. (1999) Peroxynitrite-induced reactions of synthetic oligonucleotides containing 8-oxoguanine, *Chem. Res. Toxicol. 12*, 459−466.
12. Niles, J. C., Wishnok, J. S., and Tannenbaum, S. R. (2004) Spiroiminodihydantoin and guanidinohydantoin are the dominant products of 8-oxoguanosine oxidation at low fluxes of peroxynitrite: Mechanistic studies with ^{18}O, *Chem. Res. Toxicol. 17*, 1510−1519.
13. Niles, J. C., Wishnok, J. S., and Tannenbaum, S. R. (2001) Spiroiminodihydantoin is the major product of the 8-oxo-7,8-dihydroguanosine reaction with peroxynitrite in the presence of thiols and guanosine photooxidation by methylene blue, *Org. Lett. 3*, 963−966.
14. Niles, J. C., Burney, S., Singh, S. P., Wishnok, J. S., and Tannenbaum, S. R. (1999) Peroxynitrite reaction products of 3′,5′-di-O-acetyl-8-oxo-7,8-dihydro-2′-deoxyguanosine, *Proc. Natl. Acad. Sci. U.S.A. 96*, 11729−11734.
15. Duarte, V., Gasparutto, D., Yamaguchi, L. F., Ravanat, J.-L., Martinez, G. R., Medeiros, M. H. G., Di Mascio, P., and Cadet, J. (2000) Oxaluric acid as the major product of singlet oxygen-mediated oxidation of 8-oxo-7,8-dihydroguanine in DNA, *J. Am. Chem. Soc. 122*, 12622−12628.
16. Luo, W., Muller, J. G., Rachlin, E. M., and Burrows, C. J. (2000) Characterization of spiroiminodihydantoin as a product of one-electron oxidation of 8-oxo-7,8-dihydroguanosine, *Org. Lett. 2*, 613−616.
17. Sugden, K. D., Campo, C. K., and Martin, B. D. (2001) Direct oxidation of guanine and 7,8-dihydro-8-oxoguanine in DNA by a high-valent chromium complex: a possible mechanism for chromate genotoxicity, *Chem. Res. Toxicol. 14*, 1315−1322.
18. Kornyushyna, O., Berges, A. M., Muller, J. G., and Burrows, C. J. (2002) In vitro nucleotide misinsertion opposite the oxidized guanosine lesions spiroiminodihydantoin and guanidinohydantoin and DNA synthesis past the lesions using *Escherichia coli* DNA polymerase I (Klenow fragment), *Biochemistry 41*, 15304−15314.
19. Henderson, P. T., Delaney, J. C., Gu, F., Tannenbaum, S. R., and Essigmann, J. M. (2002) Oxidation of 7,8-dihydro-8-oxoguanine affords lesions that are potent sources of replication errors in vivo, *Biochemistry 41*, 914−921.
20. Henderson, P. T., Delaney, J. C., Muller, J. G., Neeley, W. L., Tannenbaum, S. R., Burrows, C. J., and Essigmann, J. M. (2003) The hydantoin lesions formed from oxidation of 7,8-dihydro-8-oxoguanine are potent sources of replication errors in vivo, *Biochemistry 42*, 9257−9262.
21. Duarte, V., Muller, J. G., and Burrows, C. J. (1999) Insertion of dGMP and dAMP during in vitro DNA synthesis opposite an oxidized form of 7,8-dihydro-8-oxoguanine, *Nucleic Acids Res. 27*, 496−502.
22. Taioli, E., Zhitkovich, A., Kinney, P., Udasin, I., Toniolo, P., and Costa, M. (1995) Increased DNA-protein crosslinks in lymphocytes of residents living in chromium-contaminated areas, *Biol. Trace Elem. Res. 50*, 175−180.
23. Durant, J. L., Chen, J., Hemond, H. F., and Thilly, W. G. (1995) Elevated incidence of childhood leukemia in Woburn, Massachusetts: NIEHS Superfund Basic Research Program searches for causes, *Environ. Health Perspect. 103*, 93−98.
24. Costa, M. (1997) Toxicity and carcinogenicity of Cr(VI) in animal models and humans, *Crit. Rev. Toxicol. 27*, 431−442.
25. Costa, M., and Klein, C. B. (2006) Toxicity and carcinogenicity of chromium compounds in humans, *Crit. Rev. Toxicol. 36*, 155−163.
26. Hailer, M. K., Slade, P. G., Martin, B. D., and Sugden, K. D. (2005) Nei deficient *Escherichia coli* are sensitive to chromate and accumulate the oxidized guanine lesion spiroiminodihydantoin, *Chem. Res. Toxicol. 18*, 1378−1383.
27. Slade, P. G., Hailer, M. K., Martin, B. D., and Sugden, K. D. (2005) Guanine-specific oxidation of double-stranded DNA by Cr(VI) and ascorbic acid forms spiroiminodihydantoin and 8-oxo-2′-deoxyguanosine, *Chem. Res. Toxicol. 18*, 1140−1149.
28. Liu, S., Medvedovic, M., and Dixon, K. (1999) Mutational specificity in a shuttle vector replicating in chromium(VI)-treated mammalian cells, *Environ. Mol. Mutagen. 33*, 313−319.
29. Feng, Z., Hu, W., Rom, W. N., Costa, M., and Tang, M.-S. (2003) Chromium(VI) exposure enhances polycyclic aromatic hydrocarbon-DNA binding at the p53 gene in human lung cells, *Carcinogenesis 24*, 771−778.
30. Jia, L., Shafirovich, V., Shapiro, R., Geacintov, N. E., and Broyde, S. (2005) Spiroiminodihydantoin lesions derived from guanine oxidation: Structures, energetics, and functional implications, *Biochemistry 44*, 6043−6051.
31. Jia, L., Shafirovich, V., Shapiro, R., Geacintov, N. E., and Broyde, S. (2005) Structural and thermodynamic features of spiroiminodihydantoin damaged DNA duplexes, *Biochemistry 44*, 13342−13353.
32. Kornyushyna, O., and Burrows, C. J. (2003) Effect of the oxidized guanosine lesions spiroiminodihydantoin and guanidinohydantoin on proofreading by *Escherichia coli* DNA polymerase I (Klenow fragment) in different sequence contexts, *Biochemistry 42*, 13008−13018.
33. Devor, E. J., and Behlke, M. A. (2005) *Oligonucleotide Yield, Resuspension, and Storage*, Integrated DNA Technologies, Coralville, IA.

34. Cantor, C. R., Warshaw, M. M., and Shapiro, H. (1970) Oligonucleotide interactions. III. Circular dichroism studies of the conformation of deoxyoligonucleotides, *Biopolymers 9*, 1059−1077.
35. Warshaw, M. M., and Cantor, C. R. (1970) Oligonucleotide interactions. IV. Conformational differences between deoxy- and ribodinucleoside phosphates, *Biopolymers 9*, 1079−1103.
36. Vallone, P. M., and Benight, A. S. (2000) Thermodynamic, spectroscopic, and equilibrium binding studies of DNA sequence context effects in four 40 base pair deoxyoligonucleotides, *Biochemistry 39*, 7835−7846.
37. Marky, L. A., and Breslauer, K. J. (1987) Calculating thermodynamic data for transitions of any molecularity from equilbrium melting curves, *Biopolymers 26*, 1601−1620.
38. Breslauer, K. J. (1987) Extracting thermodynamic data from equilibrium melting curves for oligonucleotide order-disorder transitions, *Methods Enzymol. 259*, 221−242.
39. Liang, F., and Cho, B. P. (2007) Probing the thermodynamics of aminofluorene-induced translesion DNA synthesis by differential scanning calorimetry, *J. Am. Chem. Soc. 129*, 12108−12109.
40. Chakrabarti, M. C., and Schwarz, F. P. (1999) Thermal stability of PNA/DNA and DNA/DNA duplexes by differential scanning calorimetry, *Nucleic Acids Res. 27*, 4801−4806.
41. Plum, G. E., Grollman, A. P., Johnson, F., and Breslauer, K. J. (1995) Influence of the oxidatively damaged adduct 8-oxodeoxyguanosine on the conformation, energetics, and thermodynamic stability of a DNA duplex, *Biochemistry 34*, 16148−16160.
42. Gray, D. M., Ratliff, R. L., and Vaughan, M. R. (1992) Circular dichroism spectroscopy of DNA, *Methods Enzymol. 211*, 389−406.
43. Poklar, N., Pilch, D. S., Lippard, S. J., Redding, E. A., Dunham, S. U., and Breslauer, K. J. (1996) Influence of cisplatin intrastrand crosslinking on the conformation, thermal stability, and energetics of a 20-mer DNA duplex, *Proc. Natl. Acad. Sci. U.S.A. 93*, 7606−7611.
44. Plum, G. E., and Breslauer, K. J. (1994) DNA lesions: A thermodynamic perspective, *Ann. N.Y. Acad. Sci. 726*, 45−56.
45. Law, S. M., Eritja, R., Goodman, M. F., and Breslauer, K. J. (1996) Spectroscopic and calorimetric characterizations of DNA duplexes containing 2-aminopurine, *Biochemistry 35*, 12329−12337.
46. Tikhomirova, A., Beletskaya, I. V., and Chalikian, T. V. (2006) Stability of DNA duplexes containing GG, CC, AA, and TT mismatches, *Biochemistry 45*, 10563−10571.
47. Prabhu, N. V., and Sharp, K. (2005) Heat capacity in proteins, *Annu. Rev. Phys. Chem. 56*, 521−548.
48. Dunitz, J. D. (1995) Win some, lose some: Enthalpy-entropy compensation in weak intermolecular interactions, *Chem. Biol. 2*, 709−712.
49. Gelfand, C. A., Plum, G. E., Grollman, A. P., Johnson, F., and Breslauer, K. J. (1998) The impact of an exocyclic cytosine adduct on DNA duplex properties: Significant thermodynamic consequences despite modest lesion-induced structural alterations, *Biochemistry 37*, 12507−12512.
50. Pilch, D. S., Dunham, S. U., Jamieson, E. R., Lippard, S. J., and Breslauer, K. J. (2000) DNA sequence context modulates the impact of a cisplatin 1,2-d(GpG) intrastrand cross-link on the conformational and thermodynamic properties of duplex DNA, *J. Mol. Biol. 296*, 803−812.
51. Plum, G. E., Grollman, A. P., Johnson, F., and Breslauer, K. J. (1992) Influence of an exocyclic guanine adduct on the thermal stability, conformation, and melting thermodynamics of a DNA duplex, *Biochemistry 31*, 12096−12102.
52. Hazra, T. K., Muller, J. G., Manuel, R. C., Burrows, C. J., Lloyd, R. S., and Mitra, S. (2001) Repair of hydantoins, one electron oxidation products of 8-oxoguanine, by DNA glycosylases of *Escherichia coli*, *Nucleic Acids Res. 29*, 1967−1974.
53. Hailer, M. K., Slade, P. G., Martin, B. D., Rosenquist, T. A., and Sugden, K. D. (2005) Recognition of the oxidized lesions of spiroiminodihydantoin and guanidinohydantoin in DNA by mammalian base excision repair glycosylases NEIL1 and NEIL1, *DNA Repair 4*, 41−50.
54. Verdine, G. L., and Bruner, S. D. (1997) How do DNA repair proteins locate damaged bases in the genome, *Chem. Biol. 4*, 329−334.
55. Ganesan, A. K., Seawell, P. C., Lewis, R. J., and Hanawalt, P. C. (1986) Processivity of T4 endonuclease V is sensitive to NaCl concentration, *Biochemisty 25*, 5751−5755.
56. Francis, A. W., and David, S. S. (2003) *Escherichia coli* Mut Y and Fpg utilize a processive mechanism for target location, *Biochemisty 42*, 801−810.
57. Bennett, S. E., Sanderson, R. J., and Mosbaugh, D. W. (1995) Processivity of *Escherichia coli* and rat liver mitochondrial uracil-DNA glycosylase is affected by NaCl concentration, *Biochemistry 34*, 6109−6119.
58. Slupphaug, G., Mol, C. D., Kavli, B., Arvai, A. S., Krokan, H. E., and Tainer, J. A. (1996) A nucleotide flipping mechanism from the structure of human uracil-DNA glycosylase bound to DNA, *Nature 384*, 87−92.
59. Hollis, T., Ichikawa, Y., and Ellenberger, T. (2000) DNA bending and a flip-out mechanism for base excision for the helix-hairpin-helix DNA glycosylase, *Escherichia coli Alk A*, *EMBO J. 19*, 758−766.
60. Fromme, J. C., and Verdine, G. L. (2002) Structural insights into lesion recognition and repair by the bacterial 8-oxoguanine DNA glycosylase MutM, *Nat. Struct. Biol. 9*, 544−552.
61. Fromme, J. C., Banerjee, A., and Verdine, G. L. (2004) DNA glycosylase recognition and catalysis, *Curr. Opin. Struct. Biol. 14*, 43−49.
62. Stivers, J. T., and Jiang, Y. L. (2003) A mechanistic perspective on the chemistry of DNA repair glycosylases, *Chem. Rev. 103*, 2729−2759.
63. Cao, C., Jiang, Y. L., Stivers, J. T., and Song, F. (2004) Dynamic opening of DNA during the enzymatic search for a damaged base, *Nat. Struct. Mol. Biol. 11*, 1230−1236.
64. Mol, C. D., Parikh, S. S., Putnam, C. D., Lo, T. P., and Tainer, J. A. (1999) DNA repair mechanisms for the recognition and removal of damaged DNA bases, *Annu. Rev. Biophys. Biomol. Struct. 28*, 101−128.
65. Yavin, E., Stemp, E. D. A., O'Shea, V. L., David, S. S., and Barton, J. K. (2006) Electron trap for DNA-bound repair enzymes: A strategy for DNA-mediated signaling, *Proc. Natl. Acad. Sci. U.S.A. 103*, 3610−3614.
66. Lukianova, O. A., and David, S. S. (2005) A role for iron-sulfur clusters in DNA repair, *Curr. Opin. Chem. Biol. 9*, 145−151.
67. Pilch, D. S., Plum, G. E., and Breslauer, K. J. (1995) The thermodynamics of DNA structures that contain lesions or guanine tetrads, *Curr. Opin. Struct. Biol. 5*, 334−342.
68. Oda, Y., Uesugi, S., Ikehara, M., Nishimura, S., Kawase, Y., Ishikawa, H., Inoue, H., and Ohtsuka, E. (1991) NMR studies of a DNA containing 8-hydroxydeoxyguanosine, *Nucleic Acids Res. 19*, 1407−1412.
69. Lipscomb, L. A., Peek, M. E., Morningstar, M. L., Verghis, S. M., Miller, E. M., Rich, A., Essigmann, J. M., and Williams, L. D. (1995) X-ray structure of a DNA decamer containing 7,8-dihydro-8-oxoguanine, *Proc. Natl. Acad. Sci. U.S.A. 92*, 719−723.
70. Krosky, D. J., Schwarz, F. P., and Stivers, J. T. (2004) Linear free energy correlations for enzymatic base flipping: How do damaged base pairs facilitate specific recognition, *Biochemistry 43*, 4188−4195.

BI701502T